A simple preparation route for polysilicate titanium salt from spent titanium solutions

Bin Xu, Yingjie Zhang, Xue Li, Yao Yao, Xuesong Huang, Shubiao Xia and Peng Dong

ABSTRACT

Polysilicate titanium salt (PST) is synthesized by using spent titanium solutions and polysilicic acid (PSiA) as raw materials. PSiA could improve the aggregation ability of titanium salt flocculants and also restrain the hydrolysis of Ti^{4+} to stabilize titanium salts. Meanwhile, replacing titanium salt with spent titanium solutions could reduce the cost of PST and solve the problem of wastewater treatment in the titanium industry, which makes valuable waste regeneration possible. Scanning electron microscopy (SEM) results show the morphology transformation (sheet, spheroid, and sphere) of PST with different Ti/Si molar ratios. The formation process of PST is analyzed by Fourier transform infrared spectroscopy (FT-IR) and X-ray photoelectron spectroscopy (XPS). This study investigates the effect of Ti/Si molar ratios on PST flocculation performance in humic–kaolin water and actual domestic wastewater treatment. The in situ floc size change of PST is measured by laser particle size analyzer in humic–kaolin water treatment. Additionally, the performance of PST is comprehensively evaluated on flocculation and sedimentation ability, rapid sweep netting ability and stability. In short, the prepared PST in this study is suitable for treating wastewater with high turbidity and chemical oxygen demand (COD) in a wide range of pH values.

Key words | flocculant, in situ floc size analysis, polysilicate titanium salt (PST), spent titanium solutions, wastewater treatment

Bin Xu
Yingjie Zhang
Xue Li (corresponding author)
Yao Yao
Xuesong Huang
Peng Dong
National and Local Joint Engineering Laboratory for Lithium-Ion Batteries and Materials Preparation Technology,
Kunming 650093,
China;
Key Laboratory of Advanced Battery Materials of Yunnan Province,
Kunming 650093,
China;
and
Faculty of Metallurgical and Energy Engineering,
Kunming University of Science and Technology,
Kunming 650093,
China
E-mail: *438616074@qq.com*

Shubiao Xia
Center for Yunnan-Guizhou Plateau Chemical Functional Materials and Pollution Control,
Qujing Normal University,
Qujing 655011,
China

INTRODUCTION

It is necessary to remove organic matter from water, which could eliminate potential carcinogenic, disinfection-byproducts (DBPs) and trihalomethanes (THMs). The main part of the organic matter in natural freshwater is humic acid (HA, about 50%–90%), which might be converted to DBPs and THMs (Hu *et al.* 2006; Kazpard *et al.* 2006). HA is composed of polycyclic aromatic macromolecules and a plurality of oxygen-containing functional groups. The concentration of HA in drinking water ranges from 3 to 5 mg/L regarding chemical oxygen demand (COD) according to standards for drinking water quality (Zhao *et al.* 2011b). Coagulation and flocculation play important roles in water treatment, which could promote the sedimentation of suspended solids from small particles to large flocs and then reduce HA as a result (Lyon *et al.* 2014; Xia *et al.* 2018).

The flocculants are mainly composed of inorganic and organic chemical electrolytes. Inorganic flocculation is widely used in water treatment due to its low cost and good effect. The inorganic flocculation used in water treatment contains iron and aluminium salts, which can be hydrolyzed in water to form a positively charged colloid such as $Al(OH)_3$ or $Fe(OH)_3$ (Duan & Gregory 2003; Wei *et al.* 2018; Yang *et al.* 2019). However, hydrolyzation is too fast to control the species of floc. To resolve this problem, polysilicic acid (PSiA) chained by Si-O-Si, such as $Si_2O_3(OH)_4^{2-}$ and $Si_3O_5(OH)_5^{3-}$, is added to the iron and aluminium salt solution to prevent iron ions and aluminium ions from precipitating, and at the same time successfully increasing floc weight and size (Zouboulis & Moussas 2008; Qiu *et al.* 2011). Nevertheless, aluminum is related to some neuropathological illness such as Alzheimer's disease (Lévesque *et al.* 2000; Camacho *et al.* 2017; Santore *et al.* 2017; Katrivesis *et al.* 2019). Compared with aluminium-based flocculants, the flocculation performance

doi: 10.2166/wst.2019.383

of iron-based flocculants is usually environmentally friendly. Unfortunately, the iron-based flocculation treated water has a higher chromaticity, which will limit its wide application (Zhao *et al.* 2013).

To overcome these difficulties, many researchers have paid attention to titanium-based flocculants. Titanium(IV) salts show good flocculation performance due to their high valence (Wu *et al.* 2011; Wang *et al.* 2019). Upton & Buswell (1937) first found that $Ti(SO_4)_2$ could be used as a flocculant in water treatment in 1937. Compared with $Al_2(SO_4)_3$, $Ti(SO_4)_2$ has better performance in removing fluoride and chromaticity color in water treatment. Shon *et al.* (2007) first reported that the coagulated sludge of titanium-based flocculants could produce TiO_2, which is applied in paints, photocatalysts, electronic paper, cosmetics, and solar cells (Obee & Brown 1995). However, there are some certain drawbacks for titanium salts during water treatment, such as high hydrolysis rate and difficulty in storage and transportation, which are similar to iron and aluminium salts. Also, the pH value of the effluent is low after titanium salt treatment (Huang *et al.* 2016b). Hence, researchers have set out to prepare polytitanium salt flocculants to improve the stability of titanium salts. Zhao *et al.* (2011a, 2011b) prepared polyaluminum chloride (PACl) to treat surface water with an effective flocculant. Furthermore, PSiA includes a large number of electronegative silica species, which could improve the aggregation ability of titanium salt flocculants and also restrain the hydrolysis of Ti^{4+} to stabilize titanium salts (Dietzel 2000; Zouboulis & Moussas 2008). Huang *et al.* (2014a, 2014b) have studied the flocculation performance and floc properties of polytitanium-silicate-sulfate and polysilicate titanium salt (PST) with different Si/Ti molar ratios during water treatment. However, a large amount of titanium salt is used in the above flocculants. It is well known that titanium salt is more expensive, and the increasing cost of titanium-based flocculants will limit their application in water treatment. Moreover, presently there is no study on the preparation of titanium-based flocculants with spent titanium solutions.

For the first time, we prepare PST with spent titanium solutions directly. The flocculation performance of the PST with different Ti/Si molar ratios is studied in sodium humate–kaolin synthetic water and domestic wastewater treatment. The physical and chemical properties of PST with different Ti/Si molar ratios are characterized by scanning electron microscopy (SEM), Fourier transform infrared spectroscopy (FT-IR) and X-ray photoelectron spectroscopy (XPS). The flocculation performance is investigated through turbidity removal efficiency and COD removal efficiency. Floc properties are evaluated by floc size, flocculate speed, sedimentation ability, rapid sweep netting ability and stability.

MATERIALS AND METHODS

Preparation of PST

The spent titanium solutions used in this work are provided by Yunnan Titanium Industry Co., Ltd, of China, and come from the cold-rolled titanium plate pickling process, and the composition is mainly metal ions such as tetravalent titanium ions and strong acid solution. The composition of the spent titanium solutions is shown in Table 1. $Na_2SiO_3{\cdot}9H_2O$, H_2SO_4 and other chemicals in this work were all purchased from Shanghai Aladdin Biochemical Technology Co., Ltd, of China. The solution used in the experiment was prepared by deionized water. The PST was prepared at room temperature.

Preparation of PSiA: First $Na_2SiO_3{\cdot}9H_2O$ was dissolved in deionized water. Then the Na_2SiO_3 solution was slowly dripped into 0.15 M H_2SO_4 solution under magnetic stirring and aged for 4 h. Finally, the PSiA solution (0.12 M as SiO_2) was acquired.

Preparation of PST: Three kinds of PST with different Ti/Si molar ratios of 2, 1 and 0.5 (named as PST2, PST1, and PST0.5, respectively) were prepared by mixing PSiA with different volumes of spent titanium solutions. The experimental process is shown in Figure 1.

Preparation of sodium humate–kaolin synthetic water and domestic wastewater

Sodium humate–kaolin synthetic water was synthesized by sodium humate (purchased from Sinopharm Group Co., Ltd, Shanghai) and kaolin; 50 mg sodium humate and 5 g

Table 1 | The composition of the spent titanium solutions

Elements	Ti	Al	Ca	Fe	Mg	Si	V	NO^{3-}
Content (g L^{-1})	24.3	0.11	0.25	0.14	0.036	2.06	<0.001	195.75

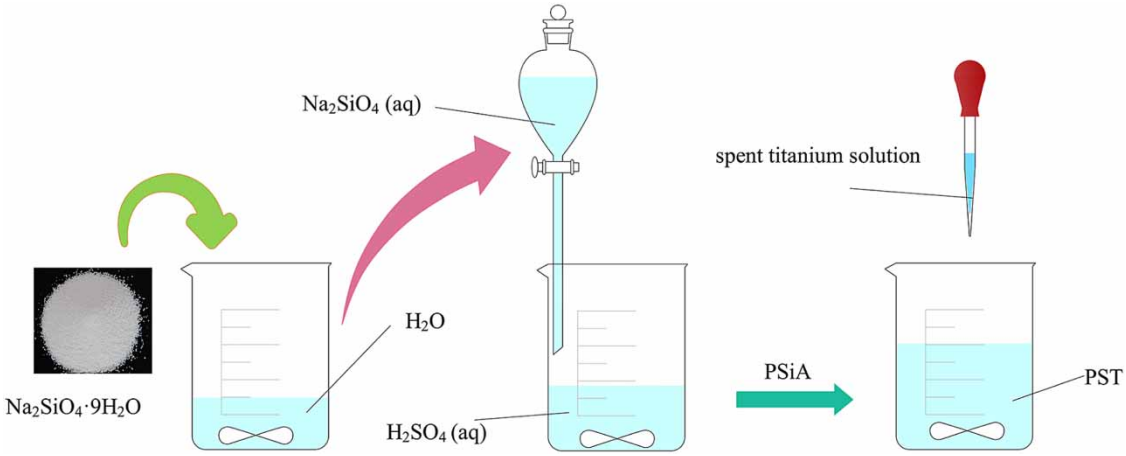

Figure 1 | The preparation process of PST.

kaolin were dissolved into 5 L deionized water under magnetic stirring for 1 h and allowed to stand for 30 min. The sodium humate–kaolin synthetic water contained 10 mg/L sodium humate with initial turbidity of 143 ± 0.5 NTU (nephelometric turbidity unit) and was adjusted by kaolin. The d50 values of kaolin used in this experiment were 1.63–3.89 μm. The COD and pH value of the sodium humate–kaolin synthetic water were 36.4 ± 0.1 mg/L and pH = 7.89 ± 0.02, respectively.

Rural domestic wastewater was collected from the Dianchi valley. The properties of the domestic wastewater were as follows: turbidity = 126 ± 1 NTU, COD = 61.1 ± 1 mg/L, pH = 7.13 ± 0.02.

Flocculation experiment

The flocculation experiment was used to evaluate the flocculation performance of PST. Initially, 250 mL of sodium humate–kaolin synthetic water and domestic wastewater was transferred to a beaker, respectively. Then, the different Ti/Si molar ratio PST was added in each beaker and the pH value was controlled from 3 to 12 with stirring (first, stirred rapidly at 200 rpm for 3 min; second, stirred slowly at 40 rpm for 10 min; finally settled for 30 min). Finally, collection was from 2 cm below the solution surface for subsequent measurements. Turbidity was directly measured without any handling using a 2100P turbidimeter (Hach, USA). COD was measured by potassium permanganate titration.

Characteristics of flocculants

The surface morphology of freeze-dried PST was observed by scanning electron microscope (TESCAN VEGA3, CZE) at an accelerating voltage of 20 kV. The PSiA and PST with different Ti/Si molar ratios were characterized by a KBr pressed disc with Fourier transform infrared spectroscopy (Thermo Scientific Nicolet iS10, USA). The chemical valence states of Ti and Si on the surface of the PST were investigated by using X-ray photoelectron spectroscopy (Thermo Fisher Scientific, K-Alpha$^+$) with a monochromatic Al X-ray source (1,486.6 eV). The particle size distribution of kaolin was tested by Mastersizer 3000 (Malvern, UK), as shown in Figure 2 and Table 2. The variation of floc size in situ during the treated sodium humate–kaolin synthetic water process was measured by Mastersizer 3000. We tested the particle size every 16 seconds and tested a total of 200 times with 500 rpm stirring speed. In this study, the floc size is represented by the median volumetric diameter (d50).

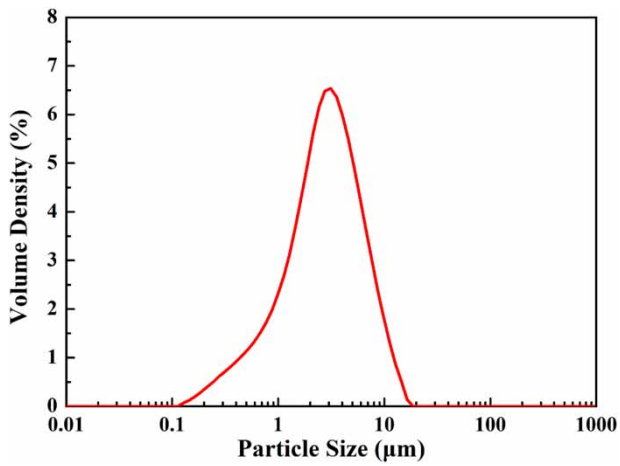

Figure 2 | The particle size distribution of kaolin.

Table 2 | The particle size of kaolin

Sample	d10 (μm)	d50 (μm)	d90 (μm)
Kaolin	0.78	2.96	7.65

RESULTS AND DISCUSSION

The morphology and surface structure of PST2, PST1, and PST0.5 were investigated by SEM as shown in Figure 3. It is clear that the Ti/Si molar ratio directly affects the overall morphology of the PST. When the Ti/Si molar ratio is 2:1, the prepared PST2 displays a rod-like structure with a width of 0.21–4.08 μm. When the Ti/Si molar ratio is 1:1, the prepared PST1 reveals a spherical shape with agglomeration and the particle diameter is about 0.61–3.31 μm. Once the Ti/Si molar ratio drops to 1:2, the morphology of PST0.5 transforms into spherical secondary particles with a diameter of 2.66–8.35 μm. In summary, the Ti/Si molar ratio determines the morphology and surface structure of PST. The PST tends to be a one-dimensional linear or two-dimensional sheet shape when the content of titanium increases. Once the content of titanium reduces, the PST will transform into a three-dimensional spherical shape with larger secondary spherical particles.

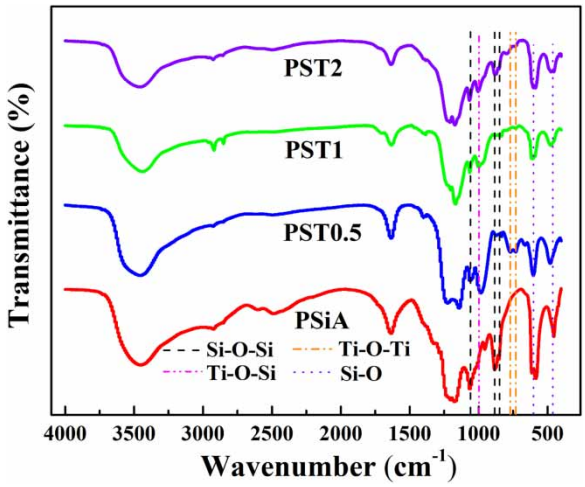

Figure 4 | FT-IR spectra of PSiA and PST with different Ti/Si molar ratios.

Figure 4 shows the FT-IR spectrum of PSiA, PST2, PST1, and PST0.5. The strong and broad peaks around 3,448 cm^{-1} and 1,635 cm^{-1} in the four samples can be attributed to the stretching vibration peak of -OH and the vibration of H_2O molecules on the material surface (Huang *et al.* 2014a; Chen *et al.* 2015a; Sun *et al.* 2017; Ajao *et al.* 2018). The vibrational bands at 1,136 cm^{-1} with strong absorptions can be ascribed to the sulfate. The absorption peaks at

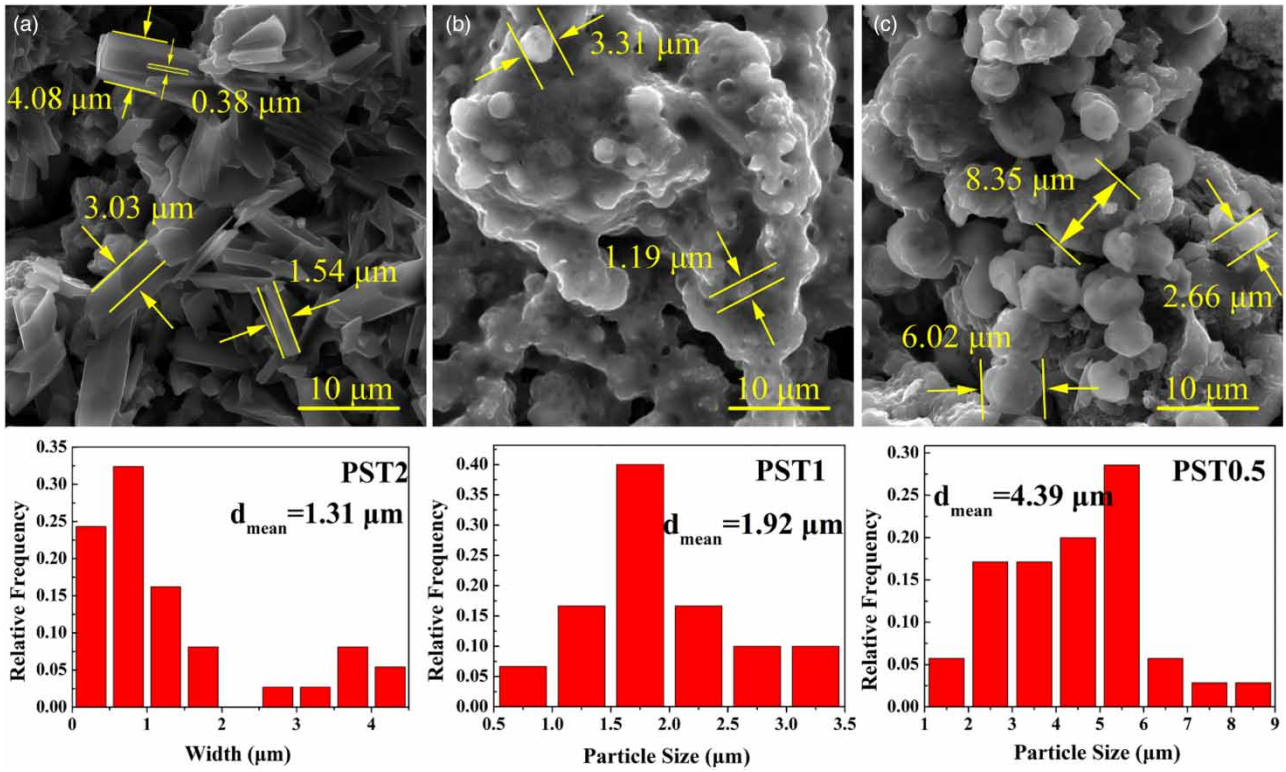

Figure 3 | SEM and size distribution images of (a) PST2, (b) PST1 and (c) PST0.5.

1,059, 884 and 848 cm^{-1} could be caused by the asymmetric stretching vibration of Si-O-Si (Moussas & Zouboulis 2008; Xu *et al.* 2009; Sun *et al.* 2017). The peak at 997 cm^{-1} corresponds to the bending vibration of Ti-O-Si, while the observed absorption band at 771 and 735 cm^{-1} could be assigned to the Ti-O-Ti stretching mode (Sun *et al.* 2010; Li *et al.* 2013; Chen *et al.* 2015b; Huang *et al.* 2016a). The absorption peaks at 601 and 462 cm^{-1} could owe to the Si-O out-of-plane bending mode and symmetry stretching mode, respectively, which stems from hydrolysis of PSiA in general (Chindaprasirt *et al.* 2009; Sun *et al.* 2017; Yan *et al.* 2017).

To analyze the bonding structure of the prepared flocculants, we detected the variation of the absorption peaks of the Si-O-Si and Ti-O-Si bonds. The results show that the intensities of both Si-O-Si and Ti-O-Si bonds experience a process of rising and then falling with the titanium content increasing. So, we believe that the polymerization of samples is strengthened then weakened. In addition, we could also confirm the variation of Ti-O-Ti and Si-O absorption peaks from the FT-IR results, which indicates that the inhibition of hydrolysis is strengthened and then weakened as well. The similar pattern may be attributed to the titanium-containing waste liquid promoting the formation of Si-O-Ti bonds and inhibiting the hydrolysis of PSiA. However, when spent titanium solution increases, the above effects are weakened, and then Ti^{4+} starts to hydrolyze (Dietzel 2000; Duan & Gregory 2003; Zouboulis & Moussas 2008; Qiu *et al.* 2011; Li *et al.* 2013; Chen *et al.* 2015a). It is well known that the flocculant will display an excellent bridging absorption capability and sweep netting ability with a larger floc size and a higher polymerization degree (François 1987; Li *et al.* 2013; Huang *et al.* 2016a, 2016b; Shahadat *et al.* 2017). Weighing the polymerization and hydrolysis, we can reach a conclusion that PST1 has the optimal polymerization and moderate hydrolysis while the polymerization of Ti and Si for PST0.5 is not sufficient.

The C, O, Ti, and Si XPS energy spectra of the prepared PST samples are shown in Figure 5. Since there is no C in

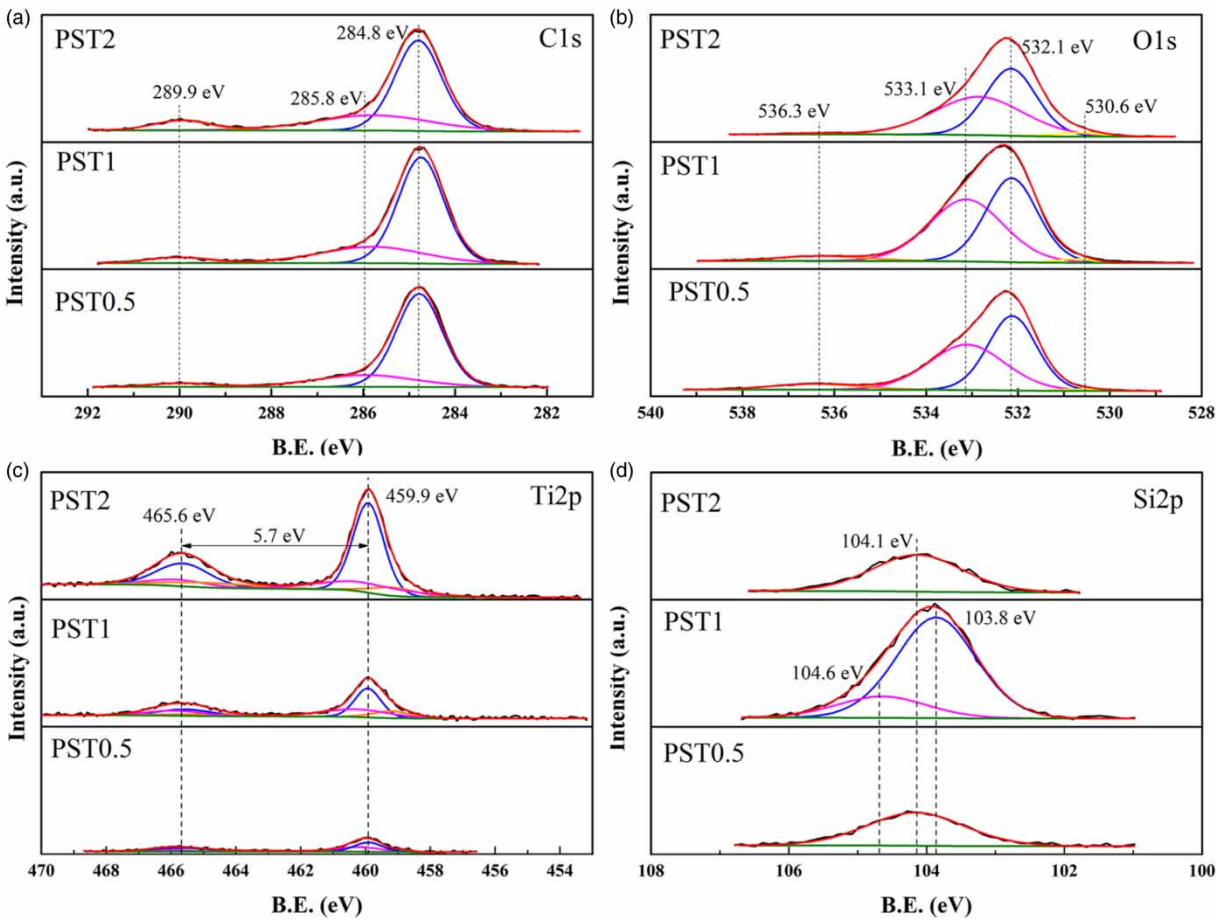

Figure 5 | XPS spectrum of (a) C1s, (b) O1s, (c) Ti2p XPS and (d) Si2p for the prepared PST (the red line represents the fitted line, the black line represents the original line, the green line represents the baseline, others are the fitting lines). Please refer to the online version of this paper to see this figure in color: http://dx.doi.org/10.2166/wst.2019.383.

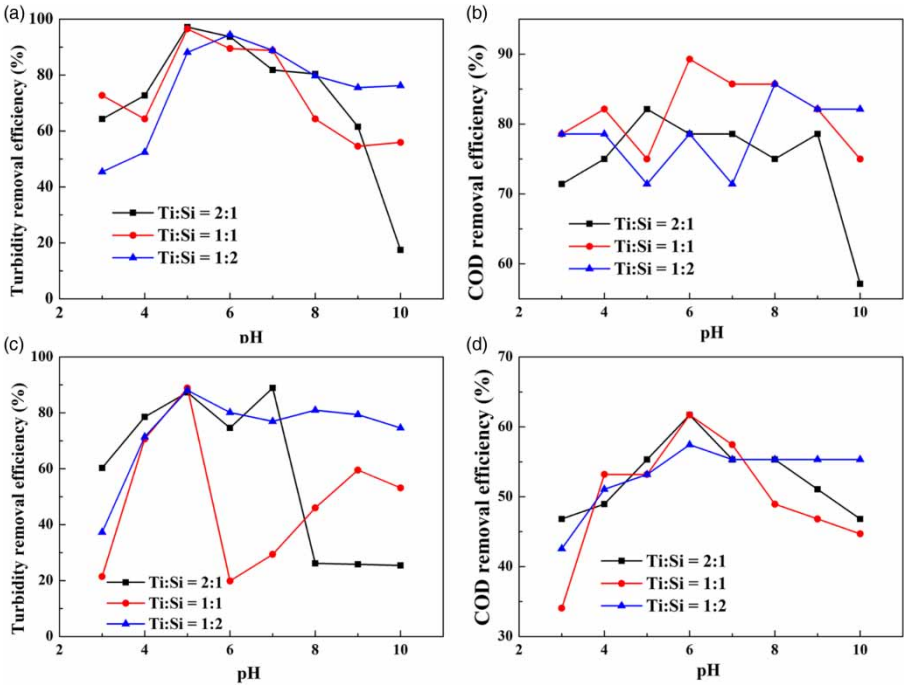

Figure 6 | Effect of solution pH on PST flocculation performance of PST2, PST1 and PST0.5: (a) turbidity removal rate and (b) COD removal rate of sodium humate–kaolin synthetic water; (c) the turbidity removal rate and (d) COD removal rate of domestic wastewater.

Table 3 | The residual turbidity, turbidity removal rate, residual COD and COD removal rate of sodium humate–kaolin synthetic water treated by different Ti/Si molar ratio PST at pH 4–6

n(Ti):n(Si)	pH	Initial turbidity (NTU)	Residual turbidity (NTU)	Turbidity removal efficiency (%)	Initial COD (mg/L)	Residual COD (mg/L)	COD removal efficiency (%)
2:1	4	143	39	72.73	36.40	9.1	75.00
	5	143	4	**97.20**	36.40	6.5	**82.14**
	6	143	9	93.71	36.40	7.8	78.57
1:1	4	143	51	64.34	36.40	6.5	82.14
	5	143	5	**96.50**	36.40	9.1	75.00
	6	143	15	89.51	36.40	3.9	**89.29**
1:2	4	143	68	52.45	36.40	7.8	78.57
	5	143	17	88.11	36.40	10.4	71.43
	6	143	8	**94.41**	36.40	7.8	**78.57**

The best performance data are marked in bold.

Table 4 | The residual turbidity, turbidity removal rate, residual COD and COD removal rate of domestic wastewater treated by PST at pH 4–6

n(Ti):n(Si)	pH	Initial turbidity (NTU)	Residual turbidity (NTU)	Turbidity removal efficiency (%)	Initial COD (mg/L)	Residual COD (mg/L)	COD removal efficiency (%)
2:1	4	126.00	27	78.57	61.1	31.2	48.94
	5	126.00	16	**87.30**	61.1	27.3	55.32
	6	126.00	32	74.60	61.1	23.4	**61.70**
1:1	4	126.00	37	70.63	61.1	28.6	53.19
	5	126.00	14	**88.89**	61.1	28.6	53.19
	6	126.00	101	19.84	61.1	23.4	**61.70**
1:2	4	126.00	36	71.43	61.1	29.9	51.06
	5	126.00	15	**88.10**	61.1	28.6	53.19
	6	126.00	25	80.16	61.1	26.0	**57.45**

The best performance data are marked in bold.

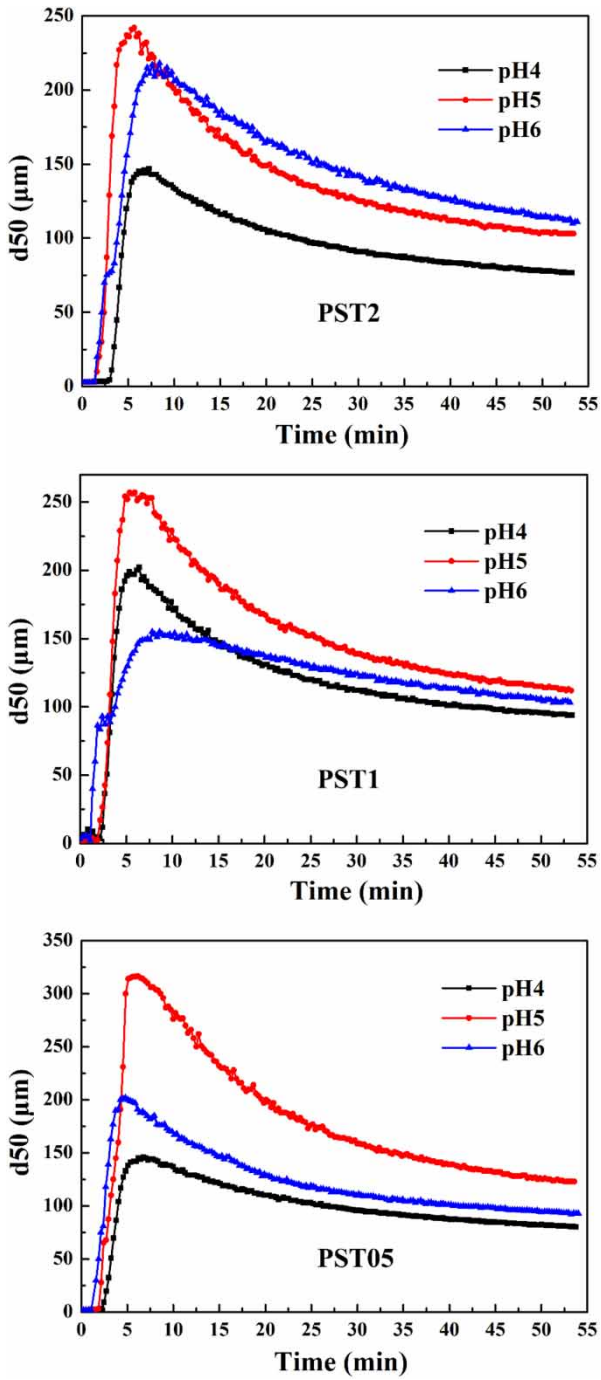

Figure 7 | Floc size change charts of PST.

the PST sample, contaminated C (CH_x) is added as a spectral alignment on the binding energy (BE) scale (284.8 eV). The C components at ~285.8 eV and ~289.9 eV of Figure 5(a) could be assigned to epoxy and carboxyl bonds, respectively (Chinh *et al.* 2018). The binding energy for the O1s peak of different Ti/Si molar ratio PST samples is mainly 532.1 eV and 533.1 eV as shown in Figure 5(b), which matches well with the state of O in TiO_2 and SiO_2 or water/OH^- (Mohai *et al.* 1990; Green *et al.* 1997). As plotted in Figure 5(c), the binding energy for the $Ti2p_{3/2}$ and $Ti2p_{1/2}$ peak of PST with different Ti/Si molar ratio samples is almost 459.9 eV and 465.6 eV, which could be contributing to the oxidation state of Ti(IV) in TiO_2, suggesting that titanium in PST is almost in a Ti(IV) state (van Hassel & Burggraaf 1991; Green *et al.* 1997; Kurtz & Henrich 1998; Hashimoto & Tanaka 2002; Oktay *et al.* 2015; Chinh *et al.* 2018). However, it is a problem that the binding energy of Ti2p is higher than in the published literature, which indicates that there is a higher valence state of Ti (TiO_x) in PST (Naitabdi *et al.* 2016; Guo *et al.* 2017; Köymen *et al.* 2019). In addition, the binding energy intensity of Ti2p XPS increases with Ti/Si molar ratio increasing, which could also indicate the Ti content rising in the PST. As shown in Figure 5(d), the binding energy for the Si2p peak of PST2, PST1 and PST0.5 is 104.1 eV, 104.1 eV and 103.8 eV, respectively, which matches well with the oxidation state of Si(IV) in SiO_2 (Oswald 2010; Philippe *et al.* 2012; Nie *et al.* 2013; Dasog *et al.* 2014).

Figure 6(a) and 6(b) and Table 3 show the turbidity and COD removal rate of sodium humate–kaolin synthetic water by PST treatment. With the increase of pH value, the PST turbidity removal efficiency first increases and then decreases. The best applicable treatment pH range for the prepared PST is from 5 to 6, and the turbidity removal efficiency and the COD removal efficiency can be as high as 94% and 78%, respectively. In comparison, PST0.5 has more stable turbidity and COD removal efficiency over a wider range of pH. With the titanium content rising, the turbidity removal efficiency is more efficient: when the Ti/Si molar ratio is 2:1 (the pH value is 5), the turbidity removal rate can be up to 97.2%. In addition, when the Ti/Si molar ratio is 1:1, the COD removal effect is the highest, which can be up to 89.29%. Figure 6(c) and 6(d) and Table 4 show the turbidity and COD removal rate of domestic wastewater treated by PST. The optimum pH values for high turbidity removal effect and COD removal effect are 5 and 6, respectively. PST1 has a smaller application range of pH for treating domestic wastewater, while PST0.5 has a wider application range of pH. In addition, PST0.5 is more stable in removing COD at different pH values. In summary, PST1 has the best turbidity removal effect, which is as high as 88.89%. And the COD removal effect is also excellent; the COD removal

rate can be as high as 61.70%.

$$\Delta d_1 = d_{\max} - d_0 \quad (1)$$

$$\Delta d_2 = d_{\Delta t2} - d_{\max} \quad (2)$$

$$k_1 = \Delta d_1 / \Delta t_1 \quad (3)$$

$$k_2 = \Delta d_2 / \Delta t_2 \quad (4)$$

In situ particle size (d50) change of flocs is shown in Figure 7, and it is obvious that the flocculant particle size first increases rapidly then decreases, and finally becomes stable during the test process. In general, the in situ particle size detection of flocs shows the following rules in water treatment: first, the particle size of flocs increases rapidly to the maximum particle size ($d_{\max}$), which can be attributed to the aggregation of flocculant particles; second, the particle size of flocs gradually decreases and tends to a constant value over time, which is related to the stirring (Jarvis *et al.* 2005; Zhao *et al.* 2011a, 2011b; Huang *et al.* 2014a; 2014b; Vajihinejad & Soares 2018). In order to evaluate the performance of flocculants more efficiently and quickly in our experiment, we believe that excellent flocculation and sedimentation ability will be obtained with the higher max floc size ($d_{\max}$). A short time (Δt_1) for getting the max obtained floc size and a fast floc size increasing rate (k_1) are both beneficial for rapidly bridging absorption and sweep netting of suspended particulates. At the same time, smaller variation (k_2) of floc size indicates excellent stability of flocculant during treatment of contaminants. According to the results from Figure 7 and Table 5, we can reach a conclusion that PST1 has a higher $d_{\max}$, k_1 and lower k_2, which indicates PST1 will have excellent flocculation and sedimentation ability, rapid physical entrapment/adsorption ability and high stability. This conclusion is in good agreement with the actual flocculation effect evaluation as above.

CONCLUSIONS

PST with different Ti/Si molar ratios (2, 1 and 0.5) was prepared with spent titanium solutions. The preparation of PST described in this article could not only solve the problem of how to treat spent titanium solutions but also reuse the valuable resources. The morphology and surface structure of different Ti/Si molar ratio PST are influenced by the content of titanium. With the decrease of titanium content, the morphology of the PST changes from a rod-like shape and finally transforms into a sphere-like shape, while spherical particles are larger when the titanium content is low. In addition, FT-IR results show that the polymerization of Si-O-Si and Si-O-Ti for PST is first strengthened and then weakened with the decrease of titanium content, and the hydrolysis of PSiA could be effectively inhibited. The change of C, O, Ti, and Si XPS energy spectra of the PST samples are basically similar, therein, the valence states of Ti and Si were IV. The performance of the flocculant is evaluated by in situ laser particle size analyzer. The related result indicated PST1 has excellent flocculation and sedimentation ability, rapid physical entrapment/adsorption ability and high stability. Moreover, PST1 also shows the best flocculation performance in sodium humate–kaolin synthetic water and domestic wastewater treatment (turbidity removal efficiency

Table 5 | The comprehensive flocculation performance analysis of PST by using in situ particle size test

	Flocculation and sedimentation ability				Rapid sweep netting ability			Stability		
n(Ti):n(Si)	pH	d_0 (μm)	Δt_1 (min)	d_{max} (μm)	Δd_1 (μm)	k_1	Δt_2 (min)	$d_{\Delta t2}$ (μm)	Δd_2 (μm)	k_2
2:1	4	3.15	4.55	147	143.85	31.62	45.95	76.6	70.4	**1.53**
	5	2.96	4.32	**242**	239.04	**55.38**	47.75	103	139	2.91
	6	2.74	7.07	218	215.26	30.46	45.40	111	107	2.36
1:1	4	3.89	4.27	202	198.11	46.43	47.00	93.9	108.1	2.30
	5	2.29	3.50	**257**	254.71	**72.77**	47.93	112	145	3.03
	6	3.01	7.53	155	151.99	20.18	44.55	103	52	**1.17**
1:2	4	2.27	4.83	146	143.73	29.74	46.97	80	66	**1.41**
	5	1.75	4.57	**316.5**	314.75	**68.92**	47.42	123	193.5	4.08
	6	1.63	3.72	202	200.37	53.91	49.25	92.8	109.2	2.22

The best performance data are marked in bold.

d_0 —— Initial particle size of sodium humate–kaolin synthetic water (μm).

d_{max} —— Maximum floc size (μm).

Δt_1 —— The time when the floc size reaches the maximum (min).

$d_{\Delta t2}$ —— The floc size after Δt_2 from d_{max} (μm).

was 96.5% and 89.29%, respectively), and high COD removal efficiency (COD removal efficiency was 89.29% and 61.70%, respectively). The excellent performance of PST1 could be attributed to the special structure, which has a large number of stable Si-O-Ti bonds.

ACKNOWLEDGEMENTS

We gratefully acknowledge the National Natural Science Foundation of China (No. 51604132 and 21965017), the Yunnan Provincial Science and Technology Major Project (No. 2018ZE002), and the Provincial Natural Science Foundation of Yunnan (No. 2017FB085 and 2018FB087).

REFERENCES

Ajao, V., Bruning, H., Rijnaarts, H. & Temmink, H. 2018 Natural flocculants from fresh and saline wastewater: comparative properties and flocculation performances. *Chemical Engineering Journal* **349**, 622–632.

Camacho, F. P., Sousa, V. S., Bergamasco, R. & Teixeira, M. R. 2017 The use of *Moringa oleifera* as a natural coagulant in surface water treatment. *Chemical Engineering Journal* **313**, 226–237.

Chen, W., Zheng, H., Teng, H., Wang, Y., Zhang, Y., Zhao, C. & Liao, Y. 2015a Enhanced coagulation–flocculation performance of iron-based coagulants: effects of PO_4^{3-} and SIO_3^{2-} modifiers. *PLoS One* **10** (9), e0137116.

Chen, W., Zheng, H., Zhai, J., Wang, Y., Xue, W., Tang, X., Zhang, Z. & Sun, Y. 2015b Characterization and coagulation–flocculation performance of a composite coagulant: poly-ferric-aluminum-silicate-sulfate. *Desalination & Water Treatment* **56** (7), 1776–1786.

Chindaprasirt, P., Jaturapitakkul, C., Chalee, W. & Rattanasak, U. 2009 Comparative study on the characteristics of fly ash and bottom ash geopolymers. *Waste Management* **29** (2), 539–543.

Chinh, V. D., Broggi, A., Di Palma, L., Scarsella, M., Speranza, G., Vilardi, G. & Thang, P. N. 2018 XPS spectra analysis of Ti^{2+}, Ti^{3+} ions and dye photodegradation evaluation of titania–silica mixed oxide nanoparticles. *Journal of Electronic Materials* **47** (4), 2215–2224.

Dasog, M., de los Reyes, G. B., Titova, L. V., Hegmann, F. A. & Veinot, J. G. C. 2014 Size vs surface: tuning the photoluminescence of freestanding silicon nanocrystals across the visible spectrum via surface groups. *ACS Nano* **8** (9), 9636–9648.

Dietzel, M. 2000 Dissolution of silicates and the stability of polysilicic acid. *Geochimica et Cosmochimica Acta* **64** (19), 3275–3281.

Duan, J. & Gregory, J. 2003 Coagulation by hydrolysing metal salts. *Advances in Colloid & Interface Science* **100–102**, 475–502.

François, R. J. 1987 Strength of aluminium hydroxide flocs. *Water Research* **21** (9), 1023–1030.

Green, S. M., Grant, D. M. & Wood, J. V. 1997 XPS characterisation of surface modified Ni-Ti shape memory alloy. *Materials Science & Engineering A* **224** (1–2), 21–26.

Guo, Y., Zhang, S., Zhu, J., Su, L., Xie, X. & Li, Z. 2017 Effects of Pt on physicochemical properties over Pd based catalysts for methanol total oxidation. *Applied Surface Science* **416**, 358–364.

Hashimoto, S. & Tanaka, A. 2002 Alteration of Ti 2p XPS spectrum for titanium oxide by low-energy Ar ion bombardment. *Surface and Interface Analysis* **34** (1), 262–265.

Hu, C., Liu, H., Qu, J., Wang, D. & Ru, J. 2006 Coagulation behavior of aluminum salts in eutrophic water: significance of Al_{13} species and pH control. *Environmental Science & Technology* **40** (1), 325–331.

Huang, X., Gao, B., Wang, Y., Yue, Q., Li, Q. & Zhang, Y. 2014a Coagulation performance and flocs properties of a new composite coagulant: polytitanium–silicate–sulfate. *Chemical Engineering Journal* **245**, 173–179.

Huang, X., Gao, B., Yue, Q., Wang, Y. & Li, Q. 2014b Effect of Si/Ti molar ratio on enhanced coagulation performance, floc properties and sludge reuse of a novel hybrid coagulant: polysilicate titanium sulfate. *Desalination* **352**, 150–157.

Huang, X., Gao, B., Yue, Q., Wang, Y. & Li, Q. 2016a Characterization and application of a novel inorganic polymer coagulant: polytitanium-silicate-chloride. *RSC Advances* **6** (30), 24898–24905.

Huang, X., Gao, B., Sun, Y., Yue, Q., Wang, Y. & Li, Q. 2016b Effects of solution pH and synthetic method on destabilization process of polytitanium-silicate-chloride. *Journal of Hazardous Materials* **311**, 230–236.

Jarvis, P., Jefferson, B. & Parsons, S. A. 2005 Breakage, regrowth, and fractal nature of natural organic matter flocs. *Environmental Science & Technology* **39** (7), 2307–2314.

Katrivesis, F. K., Karela, A. D., Papadakis, V. G. & Paraskeva, C. A. 2019 Revisiting of coagulation–flocculation processes in the production of potable water. *Journal of Water Process Engineering* **27**, 193–204.

Kazpard, V., Lartiges, B. S., Frochot, C., d'Espinose de la Caillerie, J. B., Viriot, M. L., Portal, J. M., Görner, T. & Bersillon, J. L. 2006 Fate of coagulant species and conformational effects during the aggregation of a model of a humic substance with Al_{13} polycations. *Water Research* **40** (10), 1965–1974.

Köymen, I., Göktürk, P. A., Kocabaş, C. & Süzer, S. 2019 Chemically addressed switching measurements in graphene electrode memristive devices using *in situ* XPS. *Faraday Discussions* **213**, 231–244.

Kurtz, R. L. & Henrich, V. E. 1998 Comparison of Ti 2*p* core-level peaks from TiO_2, Ti_2O_3, and Ti metal, by XPS. *Surface Science Spectra* **5** (3), 179–181.

Lévesque, L., Mizzen, C. A., McLachlan, D. R. & Fraser, P. E. 2000 Ligand specific effects on aluminum incorporation and toxicity in neurons and astrocytes. *Brain Research* **877** (2), 191–202.

Li, R., He, C. & He, Y. 2013 Preparation and characterization of poly-silicic-cation coagulants by synchronous-polymerization and co-polymerization. *Chemical Engineering Journal* **223**, 869–874.

Lyon, B. A., Cory, R. M. & Weinberg, H. S. 2014 Changes in dissolved organic matter fluorescence and disinfection byproduct formation from UV and subsequent chlorination/chloramination. *Journal of Hazardous Materials* **264**, 411–419.

Mohai, M., Bertóti, I. & Révész, M. 1990 XPS study of the state of oxygen on a chemically treated glass surface. *Surface & Interface Analysis* **15** (6), 364–368.

Moussas, P. A. & Zouboulis, A. I. 2008 A study on the properties and coagulation behaviour of modified inorganic polymeric coagulant – polyferric silicate sulphate (PFSiS). *Separation & Purification Technology* **63** (2), 475–483.

Naitabdi, A., Fagiewicz, R., Boucly, A., Olivieri, G., Bournel, F., Tissot, H., Xu, Y., Benbalagh, R., Silly, M. G., Sirotti, F., Gallet, J.-J. & Rochet, F. 2016 Oxidation of small supported platinum-based nanoparticles under near-ambient pressure exposure to oxygen. *Topics in Catalysis* **59** (5–7), 550–563.

Nie, M., Abraham, D. P., Chen, Y., Bose, A. & Lucht, B. L. 2013 Silicon solid electrolyte interphase (SEI) of lithium ion battery characterized by microscopy and spectroscopy. *Journal of Physical Chemistry C* **117** (26), 13403–13412.

Obee, T. N. & Brown, R. T. 1995 TiO_2 photocatalysis for indoor air applications: effects of humidity and trace contaminant levels on the oxidation rates of formaldehyde, toluene, and 1,3-butadiene. *Environmental Science & Technology* **29** (5), 1223–1231.

Oktay, S., Kahraman, Z., Urgen, M. & Kazmanli, K. 2015 XPS investigations of tribolayers formed on TiN and (Ti,Re)N coatings. *Applied Surface Science* **328**, 255–261.

Oswald, S. 2010 Growth studies of Ti-based films deposited on Si and SiO_2 using angle-resolved XPS. *Surface & Interface Analysis* **42** (6–7), 1289–1294.

Philippe, B., Dedryvère, R., Allouche, J., Lindgren, F., Gorgoi, M., Rensmo, H., Gonbeau, D. & Edström, K. 2012 Nanosilicon electrodes for lithium-ion batteries: interfacial mechanisms studied by hard and soft X-ray photoelectron spectroscopy. *Chemistry of Materials* **24** (6), 1107–1115.

Qiu, Z., Liu, D. & Qiu, J. 2011 Preparation of polysilicate aluminium ferric (PSFA) using effluents and its application on banknote printing wastewater treatment. *Advanced Materials Research* **393–395**, 1376–1380.

Santore, R. C., Ryan, A. C., Kroglund, F., Rodriguez, P. H., Stubblefield, W. A., Cardwell, A. S., Adams, W. J. & Nordheim, E. 2017 Development and application of a biotic ligand model for predicting the chronic toxicity of dissolved and precipitated aluminum to aquatic organisms. *Environmental Toxicology & Chemistry* **37**, 70–79.

Shahadat, M., Teng, T. T., Rafatullah, M., Shaikh, Z. A., Sreekrishnan, T. R. & Ali, S. W. 2017 Bacterial bioflocculants: a review of recent advances and perspectives. *Chemical Engineering Journal* **328**, 1139–1152.

Shon, H. K., Vigneswaran, S., Kim, I. S., Cho, J., Kim, G. J., Kim, J. B. & Kim, J.-H. 2007 Preparation of titanium dioxide (TiO_2) from sludge produced by titanium tetrachloride ($TiCl_4$) flocculation of wastewater. *Environmental Science & Technology* **41** (4), 1372–1377.

Sun, T., Liu, L., Wan, L. & Zhang, Y. 2010 Effect of silicon dose on preparation and coagulation performance of poly-ferric-aluminum-silicate-sulfate from oil shale ash. *Chemical Engineering Journal* **163** (1–2), 48–54.

Sun, J., Shi, H., Qian, B., Xu, Z., Li, W. & Shen, X. 2017 Effects of synthetic C-S-H/PCE nanocomposites on early cement hydration. *Construction & Building Materials* **140**, 282–292.

Upton, W. V. & Buswell, A. M. 1937 Titanium salts in water purification. *Industrial and Engineering Chemistry* **29**, 870–871.

Vajihinejad, V. & Soares, J. B. P. 2018 Monitoring polymer flocculation in oil sands tailings: a population balance model approach. *Chemical Engineering Journal* **346**, 447–457.

van Hassel, B. A. & Burggraaf, A. J. 1991 Oxidation state of Fe and Ti ions implanted in yttria-stabilized zirconia studied by XPS. *Applied Physics A* **52** (6), 410–417.

Wang, X., Gan, Y. & Zhang, S. 2019 Improved resistance to organic matter load by compositing a cationic flocculant into the titanium xerogel coagulant. *Separation and Purification Technology* **211**, 715–722.

Wei, H., Ren, J., Li, A. & Yang, H. 2018 Sludge dewaterability of a starch-based flocculant and its combined usage with ferric chloride. *Chemical Engineering Journal* **349**, 737–747.

Wu, Y. F., Liu, W., Gao, N. Y. & Tao, T. 2011 A study of titanium sulfate flocculation for water treatment. *Water Research* **45** (12), 3704–3711.

Xia, X., Lan, S., Li, X., Xie, Y., Liang, Y., Yan, P., Chen, Z. & Xing, Y. 2018 Characterization and coagulation–flocculation performance of a composite flocculant in high-turbidity drinking water treatment. *Chemosphere* **206**, 701–708.

Xu, X., Yu, S. L., Shi, W., Jiang, Z. Q. & Wu, C. 2009 Effect of acid medium on the coagulation efficiency of polysilicate-ferric (PSF) – a new kind of inorganic polymer coagulant. *Separation & Purification Technology* **66** (3), 486–491.

Yan, Z., Yang, H., Ouyang, J. & Tang, A. 2017 In situ loading of highly-dispersed CuO nanoparticles on hydroxyl-group-rich SiO_2-AlOOH composite nanosheets for CO catalytic oxidation. *Chemical Engineering Journal* **316**, 1035–1046.

Yang, P., Li, D., Zhang, W., Wang, N., Yang, Z., Wang, D. & Ma, T. 2019 Flocculation–dewatering behavior of waste activated sludge particles under chemical conditioning with inorganic polymer flocculant: effects of typical sludge properties. *Chemosphere* **218**, 930–940.

Zhao, Y., Gao, B., Cao, B., Yang, Z., Yue, Q., Shon, H. & Kim, J.-H. 2011a Comparison of coagulation behavior and floc characteristics of titanium tetrachloride ($TiCl_4$) and polyaluminum chloride (PACl) with surface water treatment. *Chemical Engineering Journal* **166** (2), 544–550.

Zhao, Y., Gao, B., Shon, H., Cao, B. & Kim, J.-H. 2011b Coagulation characteristics of titanium (Ti) salt coagulant compared with aluminum (Al) and iron (Fe) salts. *Journal of Hazardous Materials* **185** (2–3), 1536–1542.

Zhao, Y., Gao, B., Zhang, G., Phuntsho, S., Wang, Y., Yue, Q., Li, Q. & Shon, H. 2013 Comparative study of floc characteristics with titanium tetrachloride against conventional coagulants: effect of coagulant dose, solution pH, shear force and break-up period. *Chemical Engineering Journal* **233** (11), 70–79.

Zouboulis, A. I. & Moussas, P. A. 2008 Polyferric silicate sulphate (PFSiS): preparation, characterisation and coagulation behaviour. *Desalination* **224** (1–3), 307–316.

First received 17 June 2019; accepted in revised form 5 November 2019. Available online 19 November 2019